Modeling the Dose Rate Response and the Effects of Hydrogen in Bipolar Technologies

X. Jie Chen, *Student Member, IEEE*, Hugh J. Barnaby, *Senior Member, IEEE*, Philippe Adell, *Member, IEEE*, Ronald L. Pease, *Fellow, IEEE*, Bert Vermeire, *Member, IEEE*, and Keith E. Holbert, *Senior Member, IEEE*

***Abstract*—A physical model describing the dose rate response and the effect of hydrogen in bipolar technologies is presented. The model uses electron-hole pair recombination and competing hydrogen reactions to explain the behaviors of bipolar devices and circuits at different dose rates. Dose-rate-dependent computer simulations based on the model were performed, and the results provide excellent qualitative agreement with the dose rate data taken on both gated lateral pnp bipolar test transistors and LM193 bipolar dual-voltage comparators. The model presented in this paper can be used to explain a variety of factors that can influence device dose rate response in bipolar technologies.**

***Index Terms*—Bipolar oxide, dose rate, enhanced low dose rate sensitivity (ELDRS), hydrogen, interface traps, radiation-induced.**

I. Introduction

UNDERSTANDING the effects of dose rate, particularly enhanced low dose rate sensitivity (ELDRS), in bipolar technologies is critical to improving the performance and reliability of electronics in the low-dose-rate space environment. The metric for characterizing the dose rate response is the enhancement factor versus dose rate, which was first introduced by Johnston *et al.* [1]. The enhancement factor is defined as the response of a part specification (e.g., current gain, input bias current) at a specified total dose and dose rate normalized to the response at the same dose and a fixed maximum dose rate. This maximum rate is typically chosen to be between 100 and 1000 rd/s. Most devices and circuits that exhibit ELDRS show an enhancement factor of 1 at high dose rates (usually > 100 rd/s) and an enhancement factor that reaches an asymptote between 2 and ~ 100 at low dose rate (usually ~ 10 rd/s or less) [2]. Fig. 1 illustrates a representative enhancement factor versus dose rate curve that is observed in ELDRS bipolar devices and integrated circuits.

Observed experimentally, the total dose and dose rate response of bipolar parts can depend on a number of factors, including processing, final passivation [3], [4], pre-irradiation thermal stresses during burn-in or packaging [5], and the amount of an external source of hydrogen, e.g., in a sealed package [6]. Several models have been proposed to describe the dose rate behavior of bipolar devices and circuits [7], [9], but most of these cannot fully explain the abundance of factors that can dictate the total ionizing dose (TID) and dose rate behaviors mentioned.

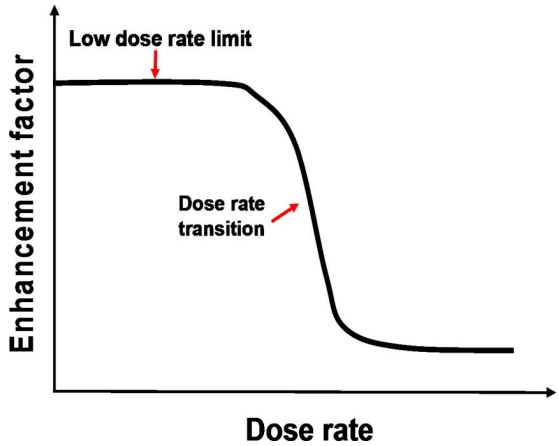

Fig. 1. Depiction showing a typical dose rate response of a bipolar circuit or device exhibiting ELDRS.

As suggested in [10], TID and dose rate effects in bipolar technologies can result from not one, but many, concurrent processes taking place during radiation exposure. As daunting as the modeling effort may seem, it is still possible to model the dose rate response with a high degree of certainty using a few core mechanisms. In this paper, the effect of dose rate is numerically modeled with four processes. These are space charge effects [7], electron-hole recombination [11], hole-hydrogen defect reactions in the oxides, and proton depassivation of dangling bonds at the Si/SiO_2 interface. The last two processes are based on the two-stage hydrogen transport model of interface trap formation developed over the years [12], [13].

II. Physical Model

When a bipolar transistor is exposed to ionizing radiation, electron-hole pairs are generated uniformly throughout the isolation oxides above the active silicon layers (primarily base region). At higher dose rates, large local E-fields in these oxides induced by substantial space charge buildup not only limit the

Manuscript received July 17, 2009; revised September 07, 2009 and September 30, 2009. Current version published December 09, 2009. This work was supported in part by the Jet Propulsion Laboratory under the NASA Electronics Parts Program (NEPP), the Air Force Office of Scientific Research under the MURI program, and the United States Department of Energy.

X. J. Chen is with Radiation Monitoring Devices, Watertown, MA 02472 USA (e-mail: JChen@rmdinc.com).

H. J. Barnaby, B. Vermeire, and K. E. Holbert are with Arizona State University, Tempe, AZ 85287 USA.

P. Adell is with the Jet Propulsion Laboratory, Pasadena, CA 91109 USA (e-mail: philippe.c.adell@jpl.nasa.gov).

R. L. Pease is with RLP Research, Los Lunas, NM 87031 USA (e-mail: rpease@rlpresearch.com).

Color versions of one or more of the figures in this paper are available online at http://ieeexplore.ieee.org.

Digital Object Identifier 10.1109/TNS.2009.2034154

transport of charged species, but they also stimulate competition of other processes that can reduce the generation of interface traps and trapped charge. Such processes include: free electron-hole recombination, trapped electrons recombining with free holes [9], and free electrons recombining with trapped holes [8]. While, relative to holes, electrons in oxides are highly mobile, because of the high localized E-fields induced at high dose rates, electrons can be confined in the oxide for extended periods. As more electrons are confined in the oxide, the probability of their being trapped and/or recombining with holes becomes higher. The model presented here treats electron-hole recombination as a core mechanism for dose rate effects.

In the model, the treatment of electron-hole recombination reaction is based on general ionic recombination theory [11], and it does not include the reactions of carrier trapping and detrapping. The recombination reaction is coupled with carrier transport (modeled as drift and diffusion) and can be described by

$$\frac{\partial p^+}{\partial t} = g_o \dot{R}_{\rm D} - \sigma_{\rm recomb} n^- p^+ - r_{\rm DH} p^+ N_{\rm DH} - \frac{\partial f_{p^+}}{\partial x} \quad (1)$$

and

$$\frac{\partial n^-}{\partial t} = g_o \dot{R}_{\rm D} - \sigma_{\rm recomb} n^- p^+ - \frac{\partial f_{n^-}}{\partial x} \quad (2)$$

where $\dot{R}_{\rm D}$ is the dose rate, g_o is the dose rate to carrier generation rate conversion factor, $\sigma_{\rm recomb}$ is the electron-hole recombination reaction coefficient, $N_{\rm DH}$ is the density of hydrogen-containing defects, $r_{\rm DH}$ is the hole-hydrogen defect reaction rate constant, and f_{n^-} and f_{p^+} are the fluxes of electrons and holes, respectively, which are modeled with drift and diffusion components as follows:

$$f_{n^-} = \mu_{n,\rm ox} n^- E_{\rm ox} + D_{n,\rm ox} \frac{dn^-}{dx} \quad (3)$$

and

$$f_{p^+} = \mu_{p,\rm ox} p^+ E_{\rm ox} - D_{p,\rm ox} \frac{dp^+}{dx} \quad (4)$$

where $\mu_{n,\rm ox}$, $\mu_{p,\rm ox}$ are electron and hole mobilities in the oxide, $D_{n,\rm ox}$ and $D_{n,\rm ox}$ are electron and hole diffusivites, and $E_{\rm ox}$ is the oxide electric field. The second key process for the proposed model is the hole-hydrogen defect reaction coupled with proton transport. This process was first proposed by [12] and can be described by the continuity equation

$$\frac{\partial H^+}{\partial t} = N_{\rm DH} r_{\rm DH} p^+ - \left[N_{\rm Si-H} - N_{\rm it}(t)\right] \sigma_{\rm it} H^+ - \frac{\partial f_{H^+}}{\partial x}, \quad (5)$$

where H^+ is the density of protons, $r_{\rm DH}$ is the hole-hydrogen defect reaction rate constant, $N_{\rm DH}$ is the density of hydrogen defects in the oxide, $N_{\rm it}$ is the density of interface traps per unit area, $N_{\rm Si-H}$ is the density of passivated dangling bonds per unit area, $\sigma_{\rm it}$ is the reaction rate constant associated with the well-known interface trap generation process between protons and passivated dangling bonds at the $\rm Si/SiO_2$ interface, and f_{H^+} is the proton flux

$$f_{H^+} = \mu_{H^+,\rm ox} H^+ E_{\rm ox} - D_{H^+,\rm ox} \frac{dH^+}{dx} \quad (6)$$

where $\mu_{H^+,\rm ox}$ and $D_{H^+,\rm ox}$ are proton mobility and diffusivity in the oxide. The term Trap generation is described by

$$\frac{\partial N_{\rm it}}{\partial t} = \left[N_{\rm Si-H} - N_{\rm it}(t)\right] \sigma_{\rm it} H^+ - \frac{N_{\rm it}(t)}{\tau_{\rm it}} \quad (7)$$

where τ_{it} is lifetime associated with the annealing of interface traps. Finally, the effect of space charge generated in the device oxide is also modeled through Poisson's equation

$$\frac{\partial E_{\rm ox}}{\partial x} = \frac{q}{\varepsilon_{\rm ox}} (p^+ - n^- + H^+) \quad (8)$$

where $E_{\rm ox}$ is the electric field and $\varepsilon_{\rm ox}$ is the permittivity of the oxide.

There are certainly other processes that likely occur during irradiation including the trapping and detrapping processes of electrons, holes and protons, the reactions of molecular hydrogen with oxygen vacancies [14], the trapping of holes at neutral sites (e.g., oxygen vacancies) and subsequent cracking of H_2 and proton release [15], the passivation reaction of silicon dangling bonds, and more. In the proposed model, these processes are not considered for simplicity, and as simulation results indicate, the core processes described in this section can still reasonably describe the dose rate response of bipolar devices. In Section III, simulation results based on the model are presented. It will also be shown that the model can explain some important factors influencing dose rate behavior, particularly the effect of irradiation bias and hydrogen concentration. It is noted here that the model described above are expressed in one dimension (1-D). However, the simulations using COMSOL Multiphysics finite-element solver were performed in two dimensions (2-D).

III. Model Simulation Versus Experimental Data

Dose-rate-dependent model simulations were carried out on a 2-D rectangular $\rm SiO_2$ structure with a thickness of 1.2 μm, approximately the same as the base isolation oxide of the bipolar devices fabricated in National Semiconductor's standard linear process [16]. The simulations were performed at dose rates ranging from 1 to 500 rd/s, all to a total dose of 30 krd.

To demonstrate the effect of $\rm electron(e^-)$-$\rm hole(h^+)$ recombination on device dose rate response, model simulations were first performed using only electrostatics and $e^- - h^+$ continuity equations for simplicity. In this case, (1)–(4) and (8) were implemented in the simulator. Using simple steady-state assumptions, the simulator calculates the flux of holes, f_{p^+}, at the $\rm Si/SiO_2$ boundary at different dose rates. The simulated hole yield, the ratio between holes coming out of $\rm SiO_2$ (escaping recombination) and total density of holes generated in $\rm SiO_2$, is plotted in Fig. 2 as a function of dose rate. Clearly indicated in the graph, the hole yield, based on the recombination model presented above, is a strong function of dose rate.

Implementing the full equation set from the model, the simulated interface trap buildup as a function of dose rate is shown in Fig. 3. To reduce the complexity of the simulation, no interface trap saturation or annealing was implemented. As shown in the figure, the interface trap dose rate response is generated for several external bias values to demonstrate the effect of applied field on the simulated response. The saturation effect at

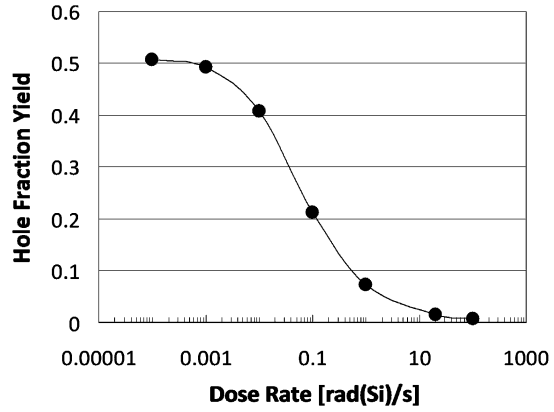

Fig. 2. Using electron-hole recombination as a core mechanism responsible for ELDRS, the hole yield produced by the simulation is strongly dependent on dose rate. The electron and hole mobilities used in the simulation are: $\mu_{n,\mathrm{ox}} = 20\ \mathrm{cm^2V^{-1}s^{-1}}$, $\mu_{p,\mathrm{ox}} = 10^{-5}\ \mathrm{cm^2V^{-1}s^{-1}}$. The recombination coefficient used is $2 \times 10^{11}\ \mathrm{cm^3/s}$.

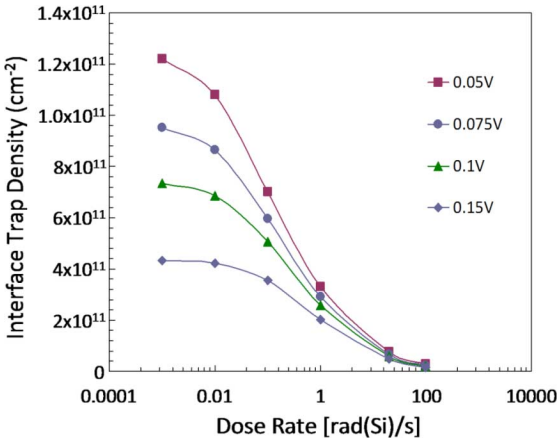

Fig. 3. Simulated interface trap density versus dose rate using the physical model described in this study. The dose rate response is also a function of applied bias, which has been observed in published data.

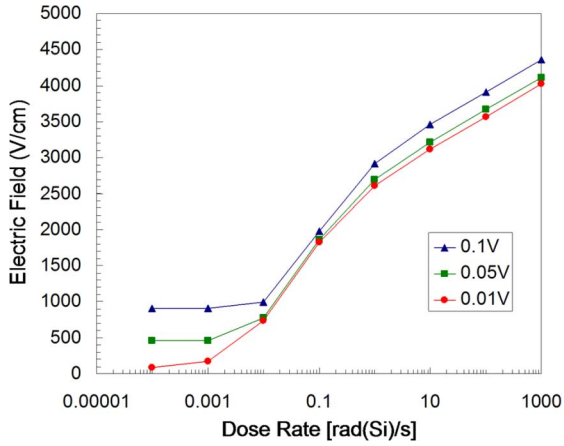

Fig. 4. Simulated average E-field (in the direction away from Si-SiO_2 interface) in the oxide showing the effect of dose rate and external bias.

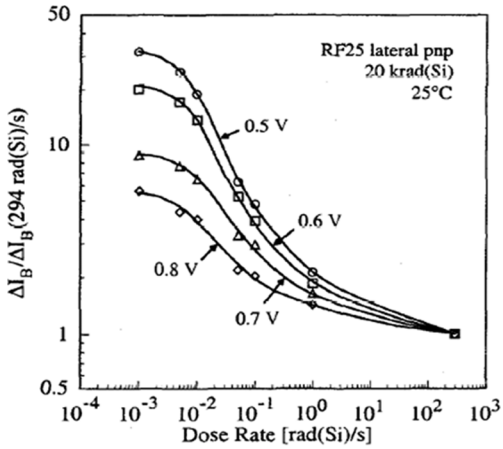

Fig. 5. Change in base current versus dose rate taken by Witczak *et al.* [17] showing ELDRS in lateral pnp bipolar devices. The dose rate responses are shown to change with base-emitter bias.

low dose rates is also correctly simulated from the model. As depicted in Fig. 4, the simulated average field across the oxide is primarily induced by radiation generated space charge at low applied biases. The internal field saturates and becomes insignificant as dose rate reaches the millirad range. At these dose rates, the magnitude of the E-field has an insignificant impact on confining electrons to recombine with holes, thus leading to greater proton generation and enhanced interface trap buildup. As the externally applied field (directed toward the SiO_2-metal interface) is increased in the simulation, the field in the oxide is changed most significantly at low dose rates, as shown in Fig. 3, and this effectively hinders the transport of positively charged species and therefore reduces the ELDRS enhancement factor.

Dose rate response data, taken by Witczak *et al.* [17], is shown in Fig. 5 for comparison. Clearly, by only using the four core processes, results shows very similar trends as the experimental data. Indeed, the model not only produces the basic ELDRS response, but it also captures the effect of external bias and shows that in devices operating with high external fields, e.g., MOS devices, the low-dose-rate enhancement can be reduced or eliminated. While Fig. 3 shows interface trap density versus dose rate and Fig. 5 gives the change of base current versus dose rate, it is well established that the radiation-induced base current is directly proportional to interface trap buildup [3]. Also, it should be noted that the biases labeled in Fig. 1 are applied at the Si-SiO_2 interface (field directed toward the gate), and the biases labeled in Fig. 3 are base-emitter voltages. The base-emitter bias can induce fringing E-fields in the base oxide producing the same bias effect as seen in the simulations.

IV. Modeling Effects of Hydrogen

As stated previously, the dose rate response of bipolar devices and circuits can depend on many factors. Devices fabricated and/or packaged in different technologies can exhibit dramatically different dose rate responses. One important feature, in common with many factors mentioned earlier, is the amount of hydrogen present in the devices. For almost every fabrication and packaging technology, hydrogen is used in one way or another to ensure proper device performance. Since hydrogen has been identified in many studies as a direct cause in degrading bipolar device TID response [18], [19], it is likely responsible

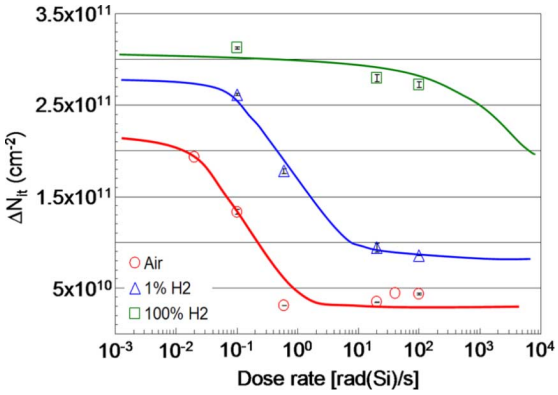

Fig. 6. $\Delta N_{\rm it}$ as a function of dose rate after irradiation in three different ambient hydrogen conditions at ASU and JPL The results indicates that dose rate response in gated lateral pnp bipolar devices can be changed by changing hydrogen concentration in the device [2].

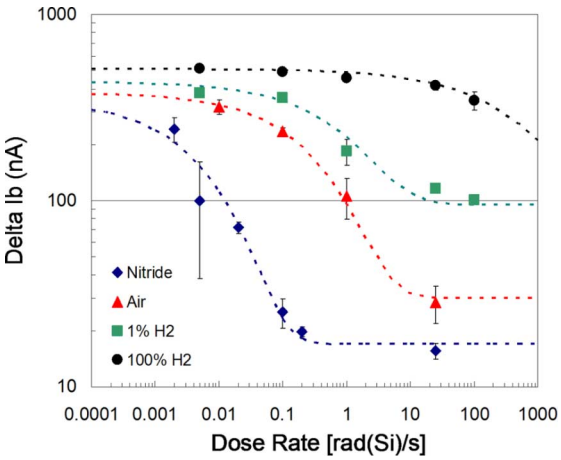

Fig. 7. Change in radiation-induced base current versus dose rate taken by JPL, showing dose rate response in LM193 bipolar dual comparator can be changed by changing hydrogen concentration in the device.

for the differences in dose rate responses of bipolar devices as well.

Recent experiments conducted at Arizona State University (ASU), Tempe, and the Jet Propulsion Laboratory (JPL), Pasadena, CA, provided clear evidence that hydrogen can directly influence the dose rate response of bipolar devices and circuits [2]. Figs. 6 and 7 show the dose rate response of a gated lateral pnp (GLPNP) bipolar test device and an LM193 bipolar dual-voltage comparator. The test devices were irradiated at different dose rates in an environment containing different concentrations of molecular hydrogen. Exhibited in both figures, the transition dose rate shifts to the right and the low dose rate limit shifts up as hydrogen concentration is increased.

Using the physical model developed for this paper, the effect of molecular hydrogen can be implemented as a disturbance to the core processes responsible for the dose rate response, particularly the recombination process of electrons and holes in (1) and (2), and the hole-hydrogen defect reaction process in (5). In recent TID studies on the effects of H_2 [14], [19], it was demonstrated that H_2 can diffuse into device oxide and react at defect centers (conceivably shallow level oxygen vacancies) to generate shallow level hydrogen defects. According to Henry's law [20],

TABLE I
LIST OF CONSTANTS USED IN THE SIMULATIONS

	Value	Unit
g_o	$8.1\text{x}10^{12}$	$\text{cm}^{-3}\text{rad}^{-1}$
r_{DH}	$2\text{x}10^{-16}$	cm^3/s
$\mu_{n,ox}$	20	$\text{cm}^2\text{V}^{-1}\text{s}^{-1}$
$\mu_{p,ox}$	10^{-8}	$\text{cm}^2\text{V}^{-1}\text{s}^{-1}$
$D_{n,ox}$	0.516	cm^2/s
$D_{p,ox}$	$2.58\text{x}10^{-10}$	cm^2/s
$\mu_{H+,ox}$	10^{-11}	$\text{cm}^2\text{V}^{-1}\text{s}^{-1}$
$D_{H+,ox}$	$2.58\text{x}10^{-13}$	$\text{cm}^2\text{V}^{-1}\text{s}^{-1}$
σ_{it}	$2.5\text{x}10^{-11}$	cm^2/s

the saturated hydrogen concentration in the bipolar oxide can be as high as 10^{18} cm^{-3}. High concentrations of hydrogen defects in the oxide can have significant impact on two key terms in the model: 1) proton generation rate; and 2) electron-hole recombination coefficient due to competition with carrier hopping [21]. The $\text{e}^- - \text{h}^+$ recombination process described in this paper is assumed to be bimolecular and, therefore, can be described by the rate equations (continuity equations) in (1) and (2). According to [21], the total rate of recombination can be attributed to two factors, one is the rate at which electrons and holes transport toward one another, and the other is the efficiency with which an electron and hole recombine at close proximity. The rate constant for bringing carriers in close proximity is defined by

$$\beta = \frac{q(\mu_n + \mu_p)}{\varepsilon_{\rm ox}} \tag{9}$$

where, according to ionic recombination theory [11], μ_n and μ_p are respective effective mobilities of electrons and holes in the oxide. The recombination efficiency is determined by the competition between carrier recombination and carrier hopping through localized defects. If it is assumed that the increase in hydrogen defects enhances competition between hopping and recombination, the overall recombination coefficient expressed in (1) and (2) can be written as

$$\sigma_{\rm recomb} \approx \beta(\mu_n, \mu_p) \cdot \eta(H_2) \tag{10}$$

where the recombination efficiency, η, is now a decreasing function of hydrogen density. Using this approach in combination with the effect of hydrogen on proton generation rate, the simulation of the effect of hydrogen on the dose rate response can be performed.

The effect of hydrogen was thus implemented in the simulator without increasing the number of simultaneous equations to minimize complexity and simulation time. This means that the model does not take into account the process of molecular hydrogen diffusion and the reaction that generates hydrogen defects. Instead, the hydrogen defect concentration, $N_{\rm DH}$ in (1) and (5), is assumed to be distributed uniformly in the oxide and increases with the molecular hydrogen concentration used during soaking experiment or during processing. For all of the simulation results presented below, applied bias across the device was zero, and the constants used are described in Table I.

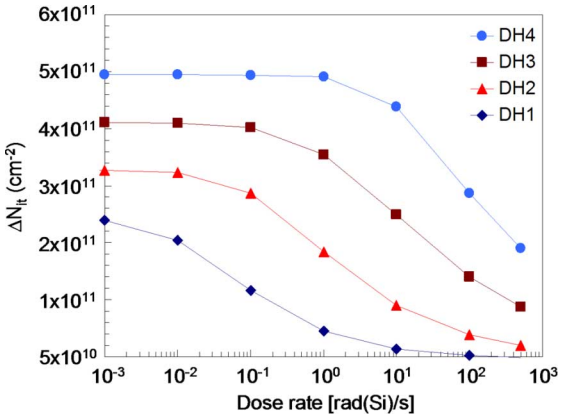

Fig. 8. The simulation results show that the effect of hydrogen on bipolar device dose rate response can be explained by the model described in this study. The results are obtained based on the theory that the e-h recombination coefficient is a function of hydrogen defect density in the oxide. The values of hydrogen densities used in the simulation are: $DH4 = 6 \times 10^{16}$ cm^{-3}, $DH3 = 5 \times 10^{16}$ cm^{-3}, $DH2 = 4 \times 10^{16}$ cm^{-3}, $DH1 = 3 \times 10^{16}$ cm^{-3}. The values of recombination coefficients used here are: $\sigma_{\text{recomb}} = 2.5 \times 10^{10}$ for DH4, 5×10^{10} for DH3, 2×10^{11} for DH2, and 2.5×10^{12} for DH1.

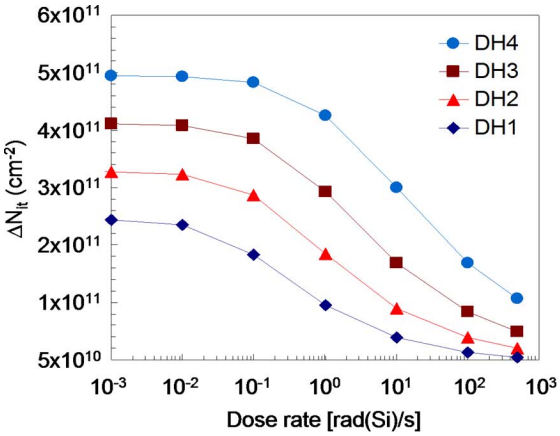

Fig. 9. These simulation results are obtained by changing the e-h recombination coefficient while keeping hydrogen defect densities the same as that of Fig. 8. The values of hydrogen densities used in the simulation are: $DH4 = 6 \times 10^{16}$ cm^{-3}, $DH3 = 5 \times 10^{16}$ cm^{-3}, $DH2 = 4 \times 10^{16}$ cm^{-3}, $DH1 = 3 \times 10^{16}$ cm^{-3}. The values of recombination coefficients used here are: $\sigma_{\text{recomb}} = 5 \times 10^{10}$ for DH4, 1×10^{11} for DH3, 2×10^{11} for DH2, and 5×10^{11} for DH1.

The results in Fig. 8 were obtained by adjusting the terms N_{DH} and σ_{recomb} accordingly, so that the increase of hydrogen defects in the device oxide reduces the $\text{e}^- - \text{h}^+$ recombination efficiency. These results correctly describe the two effects observed in the data shown in Figs. 6 and 7, i.e., the increase in the low dose rate limit and the rightward shift in transition dose rate.

Using the effect of hydrogen, the model can produce different variations of ELDRS observed in literature. By changing the hydrogen defect densities in the oxide, and/or adjusting its functional relationship with the e^--h^+ recombination coefficient in (10), different combinations of dose rate responses can be produced by the simulator.

In Fig. 9, the results are obtained by changing the recombination coefficients corresponding to each hydrogen defect concentration, while keeping the defect densities the same as the previous simulation. The results in Fig. 9 show smaller shifts in transition dose rates as hydrogen concentrations are increased. In Fig. 10, both hydrogen defect density and recombination coefficients are adjusted to reflect smaller shifts in both low dose rate limit and transition dose rates. These results simply suggest that the differences in hydrogen concentration as well as the functional relationship between hydrogen concentration and recombination coefficient can produce differences in dose rate behaviors.

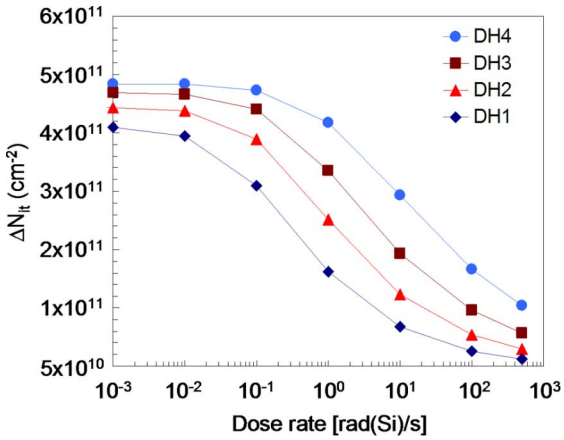

Fig. 10. These simulation results are obtained by changing both hydrogen defect densities and corresponding recombination coefficients The values of hydrogen densities used in the simulation are: $DH4 = 5.9\times10^{16}$ cm^{-3}, $DH3 = 5.7 \times 10^{16}$ cm^{-3}, $DH2 = 5.4 \times 10^{16}$ cm^{-3}, $DH1 = 5 \times 10^{16}$ cm^{-3}. The values of recombination coefficients used here are: $\sigma_{\text{recomb}} = 5 \times 10^{10}$ for DH4, 1×10^{11} for DH3, 2×10^{11} for DH2, and 5×10^{11} for DH1.

V. Discussion

The simulation results in Figs. 8 and 10 are produced by making small changes in hydrogen defect concentration and large changes in recombination coefficient. In Fig. 10, a factor of 2 difference in DH concentration (between DH1 and DH4) requires two orders of magnitude drop in recombination coefficient to produce the shifts in transition dose rates and interface trap densities similar to the data from the hydrogen soaking experiments. This means that the sensitivity of dose rate response to hydrogen defect concentration is very high, and it may not make physical sense based on previous hydrogen soaking experimental results in which the dose rate response is much less sensitive to ambient molecular hydrogen concentrations. However, one significant difference between the simulation and experimental data is the hydrogen species used. In H_2 soaking experiments, the dose rate response is measured as a function of ambient molecular hydrogen, but in model simulations, only hydrogen defects formed in the oxide are considered. It's possible that: 1) hydrogen defects formed during soaking experiments are significantly lower than ambient H_2 concentration; and 2) molecular hydrogen diffusion and reactions may also affect dose rate response through another mechanism. Because there is no conclusive physical evidence on how hydrogen affects the recombination coefficient, it is difficult to quantitatively formulate the relationship between these two parameters. The simulation results are produced by modifying these two parameters accordingly to best fit one set of experimental data. Furthermore, the model presented does not take into account the

effect of molecular hydrogen diffusion and reaction, which may provide more complete explanation for such high variations in dose rate response during H_2 soaking experiments.

Using the combined effect of electron/hole recombination and hydrogen reactions, the model presented in this paper not only explains the dependence of ELDRS on electric field, but it also covers the effect of hydrogen on dose rate response. Hydrogen effects have great implications for understanding ELDRS in bipolar devices, particularly for explaining the variations in ELDRS behaviors between many types of bipolar devices and circuits, across different fabrication and packaging technologies.

Hydrogen is the common ingredient used in many technologies. Devices fabricated in different technologies would most likely encounter different concentrations of hydrogen at different processing steps. Moreover, the differences in technology can also result in parts with drastically different oxide quality. One measure of the quality of the oxide is the density of oxygen vacancies. Because oxygen vacancies can react with hydrogen species [14], they can directly influence the amount of hydrogen defects that can be generated in the device. Furthermore, variations in processing temperature across different technologies can also influence the density of hydrogen species since oxygen vacancy formation, hydrogen diffusion, and hydrogen defect generation are all strong functions of temperature. The influence of temperature may be directly related to the dose rate response differences in devices with and without pre-irradiation thermal stress during burn-in or packaging [5]. The effect of passivation layers on dose rate response observed in [4] can also be attributed to hydrogen, as different passivation layers not only contain different concentrations of hydrogen, but some also act as barriers to hydrogen diffusion. A layer of silicon nitride, for example, can prevent hydrogen from diffusing in and out of the device oxide because molecular hydrogen diffusivity in this material is extremely low. Different passivation layers may also require different temperatures for deposition, and this again may influence the amount of hydrogen defects generated in the device oxide.

As stated earlier, most models presented in literature cannot fully explain the many different factors influencing bipolar device dose rate behavior. However, in their latest work, Hjarmalson *et al.* [15] also presented dose rate calculations using the effect of hydrogen. There are two major differences between Hjarmalson's and the calculations presented here. First, the model presented here uses conventional two-stage hydrogen transport model to calculate proton generation and interface trap buildup [12]. In this model, protons responsible for interface trap creation is generated by holes reacting with hydrogen bonded defects in the oxide

$$h^+ + DH \rightarrow D + H^+. \tag{11}$$

In Hjalmarson's calculations, protons are generated through two intermediate reactions, hole trapping and molecular hydrogen cracking, proposed by Mrstik and Rendell [22]

$$\begin{aligned} h^+ + DH &\rightarrow D^+ + H \\ H + H &\rightarrow H_2 \\ H_2 + D^+ &\rightarrow DH + H^+. \end{aligned} \tag{12}$$

The other difference is in the core mechanisms responsible for ELDRS and the effect of hydrogen. In Hjalmarson's calculations, the dose rate and hydrogen effect are due to the competition between trapped hole-electron recombination and trapped hole-molecular hydrogen reactions in (12). In the model presented here, they come from the competition between traveling hole-electron recombination and hole-hydrogen defect reaction in (11).

The results presented in this paper also have implications on our understanding of dose rate effects in MOS devices and on finding ways to mitigate dose rate effects in bipolar devices. Even though most argue that ELDRS do not exist in MOS devices because electric field in MOS gate oxides are high enough to minimize any dose-rate-dependent effects, based on this study, another factor could be the density of hydrogen defects in the MOS oxides. The dose rate response associated with high-quality, low-hydrogen defect density MOS devices may exhibit no dose rate transition until very low dose rates are reached since shifts in transition dose rates and low dose rate enhancement factor can be changed by varying the hydrogen concentration in the oxide. To minimize or eliminate ELDRS in bipolar devices, we need to improve bipolar oxide quality and reduce hydrogen defect concentrations by modifying device processing steps and recipes.

It should be noted that the physical model developed for this paper is only simulated with steady-state assumptions to reduce complexity and simulation time. The steady-state assumption is most accurate at low dose rates, but becomes less accurate at high dose rates due to dramatic changes in concentrations of species over time. Nonetheless, the simulation results are in excellent qualitative agreement with experimental data, and the physical model can be used to explain many different factors influencing the bipolar device dose rate response observed in literature.

VI. Conclusion

In this paper, a physical model based on four core mechanisms describing the dose rate response and the effect of hydrogen in bipolar technologies is presented. These core mechanisms are: space charge effect, electron-hole recombination, hole-hydrogen defect reaction in the oxide, and proton depassivation of dangling bond at the Si-SiO_2 interface. From this physical model, ELDRS in bipolar devices is closely associated with electron-hole pair recombination. Using COMSOL finite element solver, the model is simulated in 2-D with steady-state assumptions. The model simulations not only produced ELDRS behavior in strong qualitative agreement with existing data, but the results also showed the correct dose rate behavior when an external field is applied.

Exhibited in results from further simulations, as well as in data obtained from hydrogen soaking experiments, the change in hydrogen concentration in the device oxide causes shifts in low dose rate saturation limit as well as in transition dose rates. These changes provide strong evidence that variations observed in bipolar device dose rate behaviors across different technologies are due to the effects of hydrogen, the common ingredient in many fabrication and packaging technologies.

The results from this study strongly suggest that ELDRS in bipolar devices is directly related to the amount of hydrogen defects present in the device oxide. If hydrogen defect concentrations can be controlled during fabrication, packaging, and even during device operation, the effect of ELDRS can be controlled accordingly.

ACKNOWLEDGMENT

The authors are grateful to K. Reinhardt of AFOSR and S. McClure of JPL for their support.

REFERENCES

[1] A. H. Johnston, G. M. Swift, and B. G. Rax, "Total dose effects in conventional bipolar transistors and linear integrated circuits," *IEEE Trans. Nucl. Sci.*, vol. 41, no. 6, pt. 1, pp. 2427–2436, Dec. 1994.

[2] R. L. Pease, P. Adell, B. G. Rax, X. J. Chen, H. J. Barnaby, K. E. Holbert, and H. P. Hjalmarson, "The effects of hydrogen on the enhanced low dose rate sensitivity (ELDRS) of bipolar linear circuits," *IEEE Trans. Nucl. Sci.*, vol. 55, no. 6, pt. 1, pp. 3169–3173, Dec. 2008.

[3] R. L. Pease, D. G. Platteter, G. W. Dunham, J. E. Seiler, H. J. Barnaby, R. D. Schrimpf, M. R. Shaneyfelt, M. C. Maher, and R. N. Nowlin, "Characterization of enhanced low dose rate sensitivity (ELDRS) effects using gated lateral PNP transistor structures," *IEEE Trans Nucl. Sci.*, vol. 51, no. 6, pt. 2, pp. 3773–3773, Dec. 2004.

[4] M. R. Shaneyfelt, R. L. Pease, J. R. Schwank, M. C. Maher, G. L. Hash, D. M. Fleetwood, P. E. Dodd, R. A. Reber, S. C. Witczak, L. C. Riewe, J. C. Hjalmarson, B. L. Banks, B. L. Doyle, and J. A. Knapp, "Impact of passivation layers on enhanced low-dose-rate sensitivity and pre-irradiation elevated-temperature stress effects in bipolar linear ICs," *IEEE Trans. Nucl. Sci.*, vol. 49, no. 6, pt. 1, pp. 3171–3179, Dec. 2002.

[5] M. R. Shaneyfelt, J. R. Schwank, S. C. Witczak, R. L. Pease, D. M. Fleetwood, P. S. Winokur, L. C. Riewe, and G. L. Hash, "Thermal-stress effects on enhanced low-dose rate sensitivity of linear bipolar circuits," *IEEE Trans. Nucl. Sci*, vol. 47, no. 6, pt. 3, pp. 2539–2545, Dec. 2000.

[6] R. L. Pease, P. Adell, B. G. Rax, X. J. Chen, H. J. Barnaby, K. Holbert, and H. P. Hjalmarson, "The effects of hydrogen on the enhanced low dose rate sensitivity (ELDRS) of bipolar linear circuits," *IEEE Trans. Nucl. Sci.*, vol. 55, no. 6, pt. 1, pp. 3169–3173, Dec. 2008.

[7] D. M. Fleetwood, S. L. Kosier, R. N. Nowlin, R. D. Schrimpf, R. A. Reber, M. Delaus, P. S. Winokur, A. Wei, W. E. Combs, and R. L. Pease, "Physical mechanisms contributing to enhanced bipolar gain degradation at low dose rates," *IEEE Trans. Nucl. Sci.*, vol. 41, no. 6, pt. 1, pp. 1871–1883, Dec. 1994.

[8] H. P. Hjalmarson, R. L. Pease, S. C. Witczak, M. R. Shaneyfelt, J. R. Schwank, A. H. Edwards, C. E. Hembree, and T. R. Mattsson, "Mechanisms for radiation dose-rate sensitivity of bipolar transistors," *IEEE Trans Nucl. Sci.*, vol. 50, no. 6, pt. 1, p. 1901, Dec. 2003.

[9] J. Boch, F. Saigne, R. D. Schrimpf, J.-R. Vaille, L. Dusseau, and E. Lorfevre, "Physical model for the low-dose-rate effect in bipolar devices," *IEEE Trans. Nucl. Sci.*, vol. 53, no. 6, pt. 1, pp. 3655–3660, Dec. 2006.

[10] D. M. Fleetwood, R. D. Schrimpf, T. P. Sokrates, R. L. Pease, and W. D. Dunham, "Electron capture, hydrogen release, and enhanced gain degradation in linear bipolar devices," *IEEE Trans Nucl. Sci.*, vol. 55, no. 6, pt. 1, pp. 2986–2991, Dec. 2008.

[11] H. Jungblut, D. Hansen, and W. F. Schmidt, "Ion-ion recombination in electronegative gases," *IEEE Trans. Elec. Insul.*, vol. 24, no. 2, pp. 343–348, Apr. 1989.

[12] F. B. McLean, "A framework for understanding radiation-induced interface states in SiO_2," *IEEE Trans. Nucl. Sci.*, vol. NS-27, no. 6, pp. 1651–1657, Dec. 1980.

[13] P. S. Winokur, H. E. Boesch, J. M. McGarrity, and F. B. McLean, "Two-stage process for buildup of radiation-induced interface states," *J. Appl. Phys.*, vol. 50, pp. 3492–3494, 1979.

[14] I. G. Batyrev, D. R. Hughart, R. Durand, M. Bounasser, B. Tuttle, D. M. Fleetwood, R. D. Schrimpf, S. N. Rasheev, G. W. Dunham, M. Law, and S. T. Pantelides, "Effects of hydrogen on the radiation response of bipolar transistors," *IEEE Trans. Nucl. Sci*, vol. 55, no. 6, pt. 1, pp. 3039–3045, Dec. 2008.

[15] H. P. Hjalmarson, R. L. Pease, and R. A. B. Devine, "Calculations of radiation dose-rate sensitivity of bipolar transistors," *IEEE Trans. Nucl Sci.*, vol. 55, no. 6, pt. 1, pp. 3009–3015, Dec. 2008.

[16] R. L. Pease, D. G. Platteter, G. W. Dunham, J. E. Seiler, H. J. Barnaby, R. D. Schrimpf, M. R. Shaneyfelt, M. C. Maher, and R. N. Nowlin, "Characterization of enhanced low dose rate sensitivity (ELDRS) effects using gated lateral PNP transistor structures," *IEEE Trans. Nucl. Sci.*, vol. 51, no. 6, pt. 2, pp. 3773–3780, Dec. 2004.

[17] S. C. Witczak, R. C. Lacoe, D. C. Mayer, D. M. Fleetwood, R. D. Schrimpf, and K. F. Galloway, "Space charge limited degradation of bipolar oxide at low electric fields," *IEEE Trans. Nucl. Sci.*, vol. 45, no. 6, pt. 1, pp. 2339–2351, Dec. 1998.

[18] J. R. Schwank, D. M. Fleetwood, P. S. Winokur, and P. V. Dressendorfer, "The role of hydrogen in radiation-induced defect formation in polysilicon-gate CMOS devices," *IEEE Trans. Nucl. Sci.*, vol. NS-34, no. 6, pt. 1, pp. 1152–1158, Dec. 1987.

[19] X. J. Chen, H. J. Barnaby, B. Vermeire, K. Holbert, D. Wright, R. L. Pease, R. D. Platteter, G. Dunham, J. Seiler, S. McClure, and P. Adell, "Mechanisms of enhanced radiation-induced degradation due to excess molecular hydrogen in bipolar oxides," *IEEE Trans. Nucl. Sci.*, vol. 54, no. 6, pt. 1, pp. 1913–1919, 2007.

[20] J. C. Kotz and J. P. T. Treichel, *Chemistry & Chemical Reactivity*. Philadelphia, PA: Saunders College Publishing, 1999.

[21] C. Groves and N. C. Greenham, "Bimolecular recombination in polymer electronic devices," *Phys. Rev. B*, vol. 78, p. 155206, 2008.

[22] B. J. Mrstik and R. W. Rendell, "Si-SiO_2 interface state generation during X-ray irradiation and during post-irradiation exposure to a hydrogen ambient," *IEEE Trans. Nucl. Sci.*, vol. 38, no. 6, pt. 1, pp. 1101–1110, Dec. 1991.